Pediatric Radiology (2022) 52:2549–2556
https://doi.org/10.1007/s00247-022-05413-8

ORIGINAL ARTICLE

Chest computed tomography findings of ground-glass nodules with enhancing central vessel/nodule in pediatric patients with *BMPR2* mutations and plexogenic arteriopathy

Jason P. Weinman[1] · David A. Mong[1] · LaDonna J. Malone[1] · Dunbar D. Ivy[2] · Robin R. Deterding[3] · Csaba Galambos[4]

Received: 22 December 2021 / Revised: 10 May 2022 / Accepted: 31 May 2022 / Published online: 11 June 2022

Abstract

Background Germline mutation in bone morphogenetic protein type II (*BMPR2*) is the most common cause of idiopathic/heritable pulmonary hypertension in pediatric patients. Despite the discovery of this gene there are no known descriptions of the CT or CT angiography findings in these children.

Objective To correlate the clinical presentation, pathology and chest CT findings in pediatric patients with pulmonary hypertension caused by mutations in the *BMPR2* gene.

Materials and methods We performed a search to identify pediatric patients with a *BMPR2* mutation and CT or CT angiography with the clinical history of pulmonary hypertension. Three pediatric radiologists reviewed the children's CT imaging findings and ranked the dominant findings in order of prevalence via consensus.

Results We identified three children with pulmonary hypertension and confirmed germline *BMPR2* mutations, two of whom had undergone lung biopsy. We then correlated the imaging findings with histopathology and clinical course.

Conclusion All of our patients with *BMPR2* mutations demonstrated a distinct CT pattern of ground-glass nodules with a prominent central enhancing vessel/nodule. These findings correlated well with the pathological findings of plexogenic arteriopathy.

Keywords Bone morphogenetic protein type 2 receptor mutation · Chest · Children · Computed tomography · Lungs · Plexogenic arteriopathy · Pulmonary hypertension

Introduction

Pulmonary hypertension leads to significant morbidity and mortality in infants and children. The causes of pulmonary hypertension in pediatric patients are different from those in adults. In the Tracking Outcomes and Practice in Pediatric Pulmonary Hypertension (TOPP) registry, among children with confirmed pulmonary hypertension younger than 18 years about one-half of cases (57%) were idiopathic or heritable pulmonary hypertension and 36% were congenital heart disease. Pulmonary hypertension caused by lung disease or hypoxia comprised 12% of confirmed cases with brochopulmonary dysplasia (26%) and interstitial lung disease (24%), accounting for the majority of these cases. Pulmonary arterial hypertension associated with connective tissue disease (3%), human immunodeficiency virus (0%), drugs or portopulmonary hypertension (1%) were very rare in children compared to adults [1].

Heritable causes of pulmonary hypertension are characterized by remodeling of precapillary pulmonary arteries leading to increased pulmonary vascular resistance, right heart failure and death [2–4]. Mutations of bone morphogenetic protein type 2 receptor (*BMPR2*) genes that are located on chromosome 2q33 are the primary abnormalities

✉ Jason P. Weinman
jason.weinman@childrenscolorado.org

1 Department of Radiology, Children's Hospital Colorado, 13123 E. 16th Ave., Box 125, Aurora, CO 80045, USA

2 Division of Cardiology, Department of Pediatrics, Children's Hospital Colorado, Aurora, CO, USA

3 Division of Pulmonary Medicine, Department of Pediatrics, Children's Hospital Colorado, Aurora, CO, USA

4 Department of Pathology and Laboratory Medicine, Children's Hospital Colorado, Aurora, CO, USA

associated with hereditary pulmonary hypertension [3]. A meta-analysis of 1,550 adult and pediatric patients with idiopathic, heritable and anorexigen-associated pulmonary arterial hypertension from 8 cohorts demonstrated a germline mutation for *BMPR2* in approximately 80% of all familial pulmonary hypertension cases and 20% of pulmonary hypertension cases with no known family history [4]. The mean age of diagnosis of pulmonary hypertension caused by *BMPR2* mutation is 40.1 years with a standard deviation of 17.2 years [4].

Bone morphogenetic protein type 2 receptor is a member of the transforming growth factor β *(*TGFß*)*-receptor family, which binds cytokines including TGFß, bone morphogenic protein, activin, inhibin and growth differentiation factor [5]. Haploinsufficiency in which the production the *BMPR2* gene product is 50% has been shown to result in disease.

Morrell [6] suggested a mechanism of development of pulmonary hypertension related to reduction of expression of *BMPR2* in which reduction in *BMPR2* function in pulmonary endothelial cells leads to increased endothelial apoptosis. Compromise of the endothelial layers is also thought to lead to the release of TGFß, which in turn causes proliferation of pulmonary arterial smooth muscle cells [6]. In addition, the high rate of apoptosis might favor the development of monoclonal apoptotic resistant endothelial cells, leading to the formation of networks of vascular channels in the form of plexogenic lesions [6, 7].

Findings of pulmonary hypertension on chest CT include dilation of the central pulmonary arteries, tapering of peripheral pulmonary arteries, right ventricular hypertrophy and dilation, dilated bronchial arteries and mosaic attenuation of the lungs [8, 9]. A study by Compton et al. [9] established a normal ratio of less than 1.1 in pediatric patients.

In this study, our goal was to describe lung CT findings and correlate those with histopathological features in children with *BMPR2*-induced pulmonary hypertension.

Materials and methods

Following approval by the Colorado Multiple Institutional Review Board, we performed a 15-year retrospective search of the electronic medical record as well as the cardiology, radiology and pathology databases to identify pediatric patients (ages <18 years) with *BMPR2* mutation and CT or CT angiography at Children's Hospital of Colorado with the clinical history of pulmonary hypertension. We identified three children who had at least one CT or CT angiography available for review. All three children had pulmonary hypertension confirmed on catheterization as defined by a mean pulmonary artery pressure ≥25 mmHg [1]. Two of the children had lung biopsy.

A total of seven CTs were performed in our three patients. Patient 1 had a CT angiography and two CTs with contrast agent; Patient 2 had two CT angiographies and one CT without contrast agent; and Patient 3 had one CT angiography. All CTs and all CT angiographies were performed on a Flash dual-source CT scanner (Siemens Healthcare, Erlangen, Germany). CT and CT angiography protocols utilized CARE Dose 4D dose modulation with a kilovoltage (kV) of 100 for CT and 80 for CT angiography, a quality reference milliamperes (mAs) of 70 for CT and 100 for CT angiography, a rotation time of 0.28 s, a pitch of 3 and a collimation of 128×0.6 mm. All studies were performed without anesthesia during inspiration.

We recorded the children's demographics, catheterization data, echocardiogram results, desaturation with 6-min walk, comorbidities, treatment and outcome for each child.

Three pediatric radiologists reviewed the CT images (D.A.M. with 14 years of experience, L.J.M. with 7 years of experience and J.P.W. with 12 years of experience). We achieved consensus rating of the imaging findings using the system described by Brody et al. [10] and previously used by the authors [10–13]. In addition, we recorded whether there were ground-glass nodules with a central prominent vessel/enhancing nodule because it became clear upon review of these studies that this was a common finding. We also measured the main pulmonary artery (MPA)-to-aorta ratio as described by Compton et al. [9]. We correlated the histopathological features with CT findings in Patients 1 and 2. No lung histopathology of Patient 3 was available.

Results

Clinical findings

All three patients were girls; all three died. The median age at time of first CT was 11 years (range: 4–12 years). Two of the three girls had undergone biopsy and/or autopsy; Patient 1 had two biopsies, both at 4 years of age, and underwent autopsy at 8 years of age. Patient 2 did not have lung biopsy and underwent autopsy at 12 years of age. No biopsy or autopsy was performed in Patient 3.

All three girls were born at full term without complications. None had known comorbidities at the time of presentation. None of the girls had a history of congenital heart disease. All of the girls had severe pulmonary artery hypertension with a median mean artery pressure on initial catheterization of 80 mmHg (range 64–95 mmHg). Patient 1 presented at 4 years of age with decreased activity and cough. Patient 2 presented at 11 years of age with decreased exercise tolerance. Patient 3 was treated for 2.5 years for exercise intolerance presumed to be caused by asthma before being diagnosed with pulmonary hypertension at 11 years of age.

Patient 1 underwent an atrial septostomy at 4 years of age. Patient 3 received a Potts shunt between the left pulmonary artery and the descending aorta at 12 years of age.

All three girls died related to unresponsive pulmonary hypertension. Patient 1 died of complications of pulmonary hypertension/respiratory distress at an outside facility. Patient 2 died of intracranial hemorrhage after requiring emergent venoarterial extracorporeal membrane oxygenation (ECMO) cannulation for worsening heart failure with respiratory decompensation. Patient 3 died of pulmonary hemorrhage caused by pulmonary hypertension.

The girls' initial presentation, outcome, mean pulmonary artery pressure at initial catheterization, desaturation with 6-min walk, room air saturation and medications are summarized in Table 1.

Computed tomography findings

The most common finding in all three girls was ill-defined ground-glass pulmonary nodules. Many of the nodules had a similar appearance characterized by a prominent vascular hyperenhancing nodule surrounded by a ground-glass density (Figs. 1, 2 and 3). Maximum-intensity projection reconstructions suggested that many of these nodules were connected to the pulmonary arteries by small branches that extended from the pulmonary arteries at 90° angles (Figs. 2 and 4).

In addition, patient 1 had scattered solid nodules, one of which was calcified. Partially calcified mediastinal lymphadenopathy was also present (Fig. 1). Diffuse, although relatively subtle, interlobular septal thickening was present in all three girls. Common findings of pulmonary hypertension including enlargement of the main pulmonary artery and branch pulmonary arteries and tortuosity of the pulmonary artery branches were present in all patients. All of the girls had a pulmonary artery ratio that was significantly higher than the normal value of 1.1 (Table 2) established by Compton et al. [9].

Patients 1 and 3 each had three CT studies. The constellation of findings stayed relatively consistent over the time course of the studies. Of note, Patient 3 had surgical changes of a Potts shunt (left pulmonary artery to descending aorta anastomosis) approximately 6 weeks after her first CT angiography at 12 years of age and approximately 2 years before her second CT. While the type and distribution of findings was consistent between these studies, the nodules with surrounding ground-glass halo were decreased in attenuation on the second non-contrast CT. The girl had a third CT angiography 1 week after the second, which showed more prominent ground-glass nodules and central enhancing nodules (Fig. 3).

The pathological findings of plexogenic arteriopathy suggesting systemic vessel origin [14] prompted us to study the bronchial vasculature. We found enlarged bronchial vessels (≥2 mm) in all patients. In addition, we found transpleural connections between peripheral pulmonary artery branches and pleural-based bronchial arteries in Patient 3 (Fig. 4).

Table 1 Patient characteristics

	Initial presentation	Outcome	mPAP on initial catheterization	Desaturation with 6-min walk?	Room air saturation	Pulmonary hypertension medications
Patient 1	4-year-old girl presented with 6 weeks of decreased activity and 3 weeks of cough	Deceased (8y)	95 mmHg (7 days after initial CT)	No (93%) (3 y after initial CT)	98%	Ambrisentan Furosemide Mycophenolate mofetil Prednisone Treprostinil
Patient 2	11-year-old girl presented with decreased exercise tolerance	Deceased (11y)	64 mmHg (7 months prior to initial CT)	Yes (89%) (1 m prior to initial CT)	95%	Bosentan Digoxin Furosemide Sildenafil Spironolactone Treprostinil
Patient 3	11-year-old girl with 2½-year history of exercise-induced fatigue, initially diagnosed and unsuccessfully treated for asthma	Deceased (14y)	80 mmHg (2 days after initial CT)	No, performed on 2 L O_2 (1 y prior to initial CT)	99%	Digoxin Furosemide Spironolactone Tacrolimus Tadalafil Treprostinil

CT computed tomography, *m* months, *mmHG* millimeters mercury, *mPAP* mean pulmonary artery pressure, *y* years

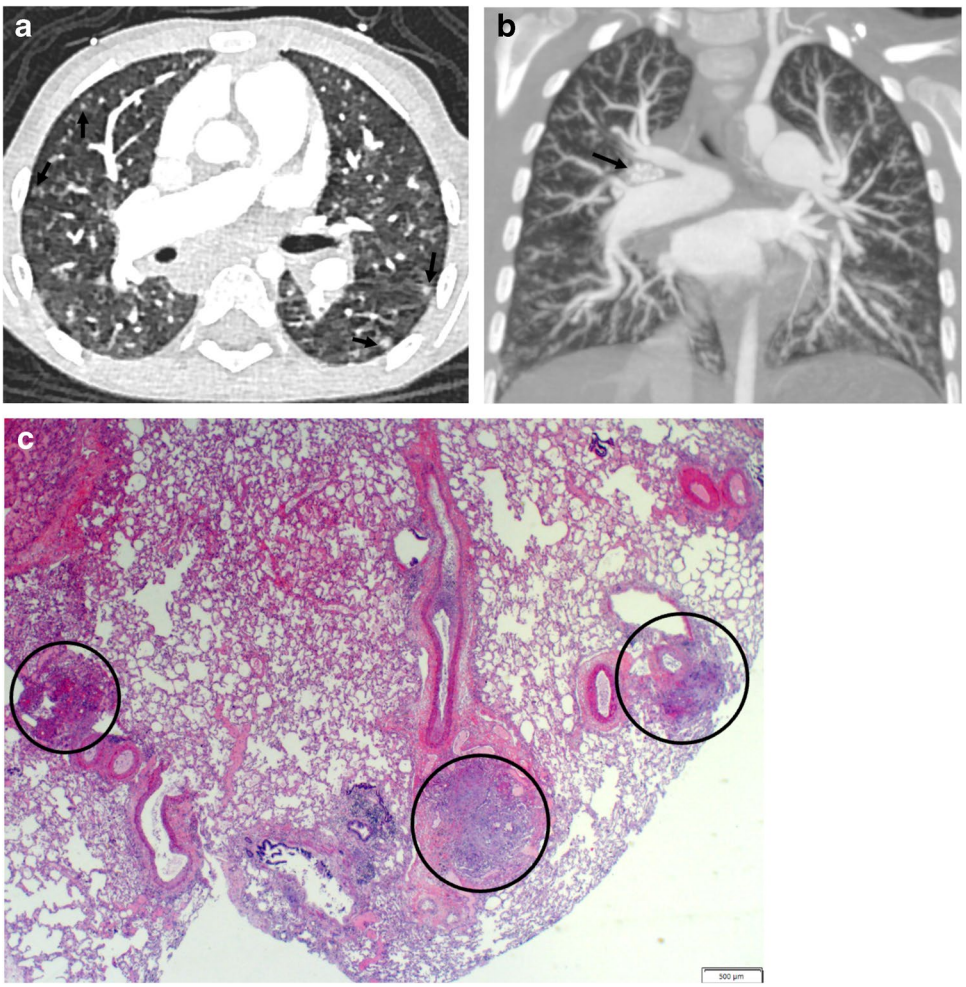

Fig. 1 Pulmonary hypertension in a 4-year-old girl with *BMPR2* mutation (Patient 1). **a** Axial CT angiogram of the chest demonstrates multiple ground-glass nodules throughout the chest with prominent central vessels (*arrows*). **b** Coronal maximum-intensity projection reconstruction of the CT angiography demonstrates tortuosity and engorgement of the pulmonary arteries with associated peripheral nodularity, as well as calcified right hilar adenopathy (*arrow*). **c** Histology. Stained section (hematoxylin and eosin ×2) demonstrates multiple plexogenic lesions (*circles*)

Pathology findings

Patient 1 underwent two lung biopsies and an autopsy. The first lung biopsy was a thoracoscopic biopsy of the left upper lobe at 4 years of age and revealed findings of plexogenic arteriopathy. A repeat open biopsy of the right upper lobe and right lower lobe were performed approximately a month later because of persistent concern for an infectious or granulomatous process given the presence of calcified nodules and lymphadenopathy. The repeat biopsy showed no infection but many pulmonary arteries with plexogenic lesions. At autopsy, Patient 1 had diffuse plexogenic arteriopathy with necrotizing vasculitis, focal pulmonary vein thickening and complex vascular lesions of the pleura (spider nevi).

At autopsy Patient 2 also had severe plexogenic pulmonary arteriopathy with complex proliferative lesions of the pleura (spider nevi).

Discussion

The CT findings of plexogenic arteriopathy are sparsely described in the literature [8]. We know of no prior description of the CT appearance of plexogenic arteriopathy or *BMPR2* mutation in pediatric patients.

In this study we describe the CT findings of *BMPR2*-mutation-related pulmonary hypertension in three children and correlated these with histopathological features in the two children for whom pathology was available. The most prevalent finding in all of our patients was diffuse ground-glass nodules with a prominent vascular hyperenhancing nodule within the center of the ground-glass nodule. Based on our correlation with histological findings, we think that ground-glass nodules with prominent central vascular hyperenhancing nodules are plexogenic lesions of pulmonary arteries. In addition, reconstructed maximum-intensity projection reconstructions demonstrated tiny vessels branching

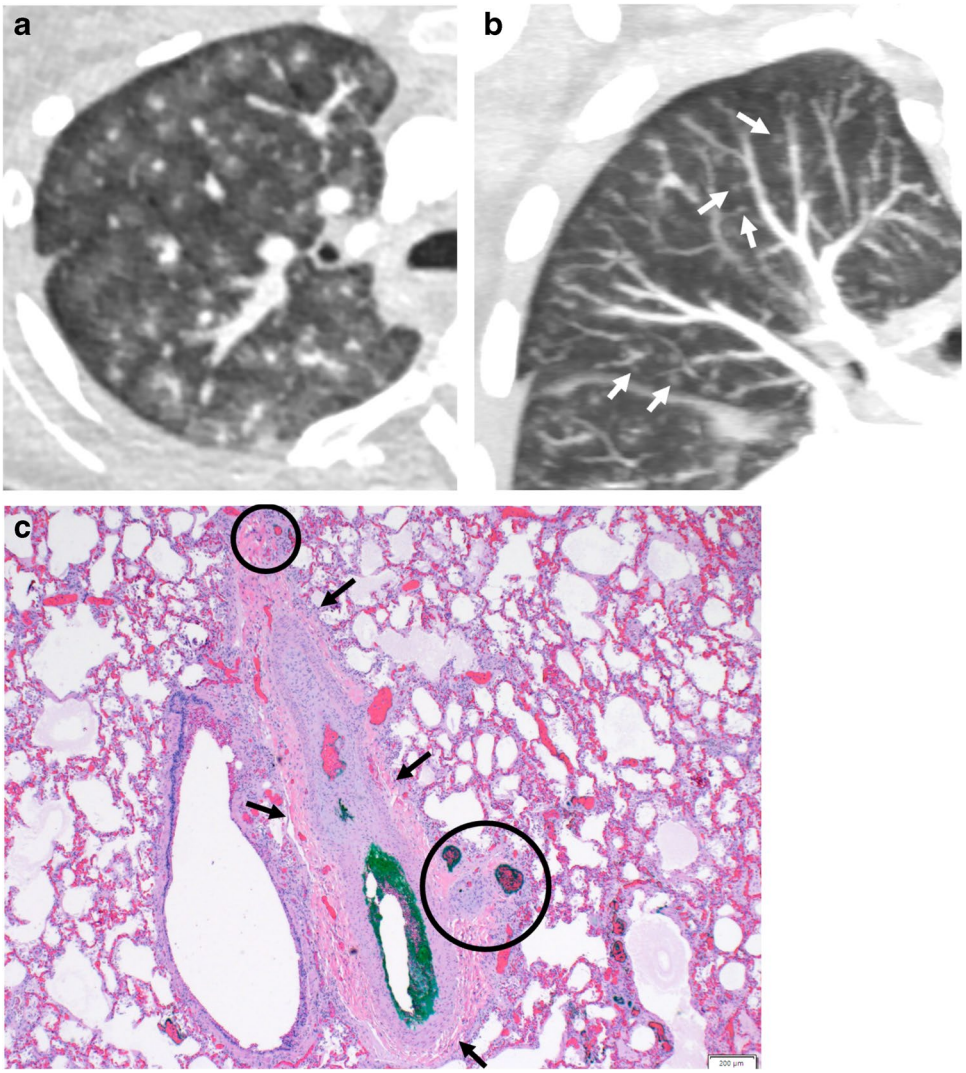

Fig. 2 Pulmonary hypertension in an 11-year-old girl with *BMPR2* mutation (Patient 2). **a** Axial CT angiogram of the right upper lobe demonstrates multiple ground-glass nodules with prominent central vessels. **b** Coronal maximum-intensity projection reconstruction of CT angiography demonstrates tiny hyperenhancing nodules (*arrows*, plexogenic lesions) extending at right angles from the pulmonary arteries, some of which appear to be connected by tiny vessels (supernumerary pulmonary arteries). **c** Histology. Hematoxylin and eosin stain (×4) with green dye injected into pulmonary artery (*arrows*). Green dye demonstrates lumen. Plexogenic lesion (*circles*) is associated with thick-walled pulmonary artery. Note that the plexogenic lesion appears to extend at right angles relative to the pulmonary artery

from the pulmonary arteries at 90° angles that connect to the hyperenhancing nodules (Fig. 2) as well as tiny branches of the peripheral pulmonary arteries that appear to extend to the pleural bronchial arteries. This suggests the presence of supernumerary pulmonary arteries [15, 16] or remodeled intrapulmonary bronchopulmonary anastomoses [14, 17].

Interestingly, Patient 3 had an increase in the severity of the ground-glass nodules between her second non-contrast CT and a repeat CT angiography 1 week later. Although the etiology of this rapid change in appearance is unclear, we think this represents enhancement of the vascular plexogenic lesion because the ground-glass nodules with central vessel/hyperenhancing nodule finding correlates with findings of plexogenic arteriopathy. Alternatively, the girl's pulmonary hypertension might have increased between the two studies, worsening the finding on the CT angiography. Unfortunately, no intercurrent echocardiogram, catheterization or pathology is available to help discriminate among these hypotheses or suggest an alternative etiology.

Review of pathology in Patient 2 revealed evidence of communication of the plexogenic lesions with bronchial circulations, as has been reported [14, 17]. All of the patients had enlarged bronchial vessels with maximum diameter greater than 2 mm and subtle communication between the peripheral pulmonary arteries and pleural vessels, which, given enlargement of the central bronchial arteries, are favored to reflect bronchial artery branches (Fig. 4). This correlates well with the pathological findings of pleural-based complex vascular lesions. Pleural-based complex vascular lesions as well as plexogenic lesions have been described in hepatopulmonary syndrome and portopulmonary hypertension [18, 19]. The communication between pulmonary and bronchial vasculature has been described in people with pulmonary arterial hypertension caused by *BMPR2* mutations that also showed bronchial artery dilation, hypertrophy and increased bronchial microvascular density [20].

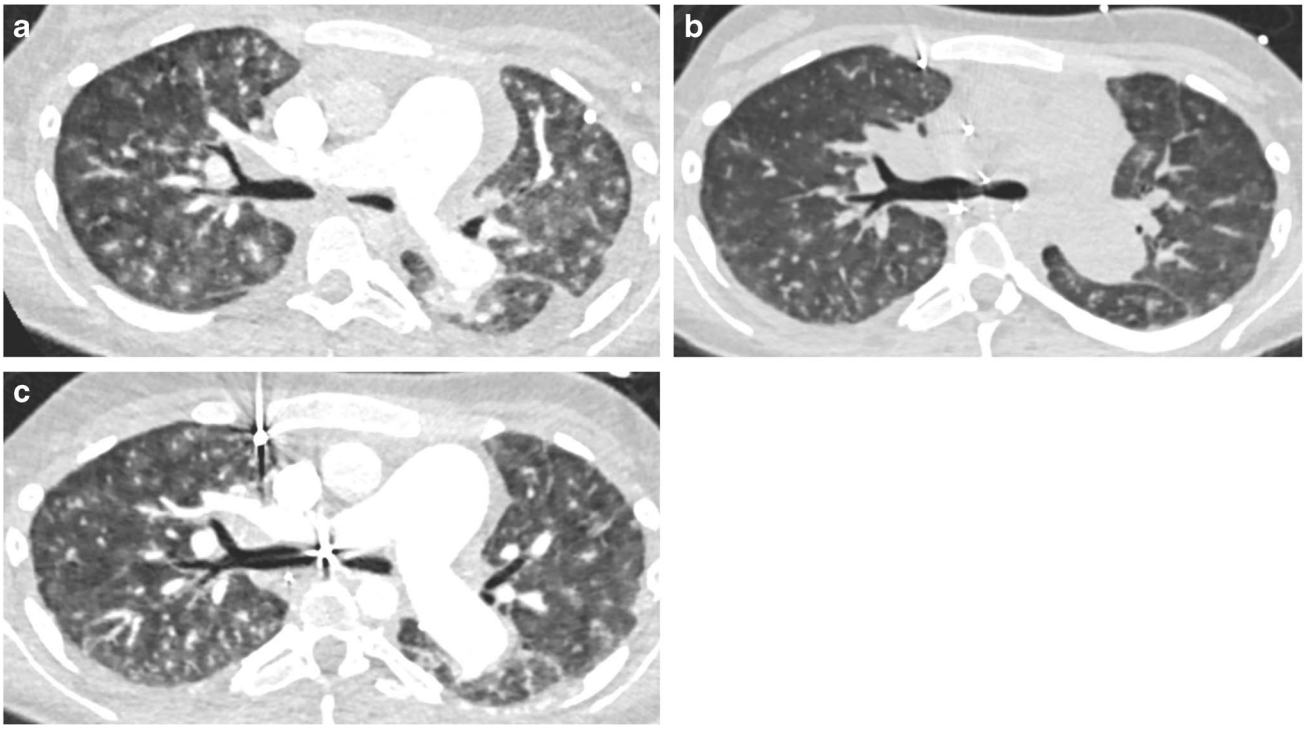

Fig. 3 Pulmonary hypertension in girl with *BMPR2* mutation (Patient 3). **a** Axial CT angiogram of the chest at age 12 demonstrates multiple ground-glass nodules throughout the chest with prominent central vessels. **b** Axial non-contrast CT in the same girl at age 14 years, about 2 years after she received a Potts shunt (left pulmonary artery to descending aorta, not shown), demonstrates decreased prominence of the ground-glass nodules with prominent central vessels compared to the first CT angiography. **c** Axial CT angiogram of the chest 1 week after (**b**) demonstrates increased conspicuity of ground-glass nodules compared to (**b**), with similar imaging findings to initial CT angiography (**a**)

We also observed relatively subtle interlobular septal thickening in all patients. Again, although we did not perform formal correlation, this could correspond to the peripheral dilated bronchial and pulmonary vessels seen on histopathology. Alternatively, this could reflect edema within the interstitial space; however, this was not demonstrated on histology.

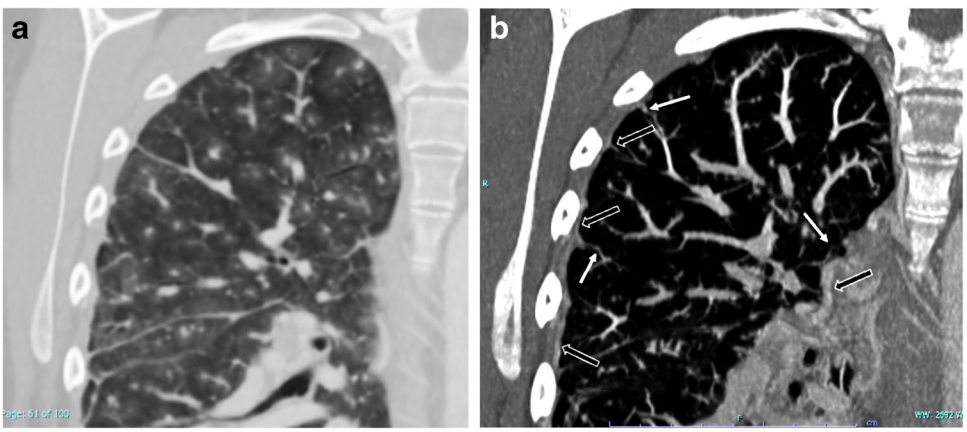

Fig. 4 Pulmonary hypertension in a 12-year-old girl with *BMPR2* mutation (Patient 3, same as in Fig. 3). **a** Coronal 1-mm CT angiogram of the chest demonstrates multiple ground-glass nodules throughout the chest with prominent central enhancing nodules (plexogenic lesions). **b** Coronal 5×1-mm maximum-intensity projection reconstruction of the same CT angiogram demonstrates enlarged central and pleural bronchial arteries (*black arrows*) with tiny vessels extending from the peripheral pulmonary arteries to the pleural based bronchial arteries (*white arrows*). Also demonstrated are tiny vessels (supernumerary pulmonary arteries) branching at right angles to pulmonary arteries with associated tiny nodules (plexogenic lesions)

Table 2 CT findings

Patient	Age at CT	Gender	Genetic mutation	MPA:Ao ratio	Findings on initial CT (in order of prevalence)	Histopathology
Patient 1	4 y, 4 y, 8 y	F	*BMPR2* and *SMAD9*	1.6	Ground-glass nodules with prominent central vessel (diffuse) Scattered more solid nodules and one calcified nodule Mediastinal adenopathy, partially calcified Interlobular septal thickening (diffuse)	Thoracoscopic biopsy LUL: age 4 y (8 days after initial CT), plexogenic arteriopathy Open lung biopsy RUL, RLL: age 4 y (1 m following CT), severe pulmonary arteriopathy with marked cellular intimal proliferation and early plexiform lesions, intra-alveolar fibrin and foamy macrophages Autopsy: age 8 y (4 y after initial CT), diffuse plexogenic arteriopathy with necrotizing vasculitis, focal pulmonary vein thickening, pleural proliferative lesions (spider nevi)
Patient 2	11 y	F	*BMPR2*	1.5	Ground-glass nodules with prominent central vessel (diffuse) Interlobular septal thickening Pleural effusion (moderate right) Cardiomegaly	Autopsy: 11 y old, severe plexogenic pulmonary arteriopathy, focal hemorrhage, many pleural spider nevi with dilated bronchial and pulmonary vasculature
Patient 3	12 y, 14 y, 14 y	F	*BMPR2*	1.9	Ground-glass nodules with prominent central vessel (diffuse) Consolidation (LLL) Pleural effusion (small left) Interlobular septal thickening Cardiomegaly	None

Ao aorta, *BMPR2* bone morphogenetic protein type 2 receptor, *CT* computed tomography, *LLL* left lower lobe, *LUL* left upper lobe, *m* months, *MPA* main pulmonary artery, *RLL* right lower lobe, *RUL* right upper lobe, *SMAD9* mothers against decapentaplegic homolog 9, *y* years

Overall, these findings suggest that plexogenic lesions play a role in shunting between the pulmonary and systemic circulation in children with severe pulmonary hypertension, such as our cohort with *BMPR2* mutations. This might explain the desaturation with exercise in some of these children without intracardiac shunts.

One of our patients (Patient 1) had partially calcified mediastinal adenopathy, solid nodules and one calcified nodule on CT. The possibility of granulomatous disease complicated by mediastinal fibrosis was posited on the CT reports. Although the girl underwent two lung biopsies as well as an autopsy, no evidence of a granulomatous process or infection was discovered and the pathogenesis and significance of this finding remains unclear.

This study is limited by its small sample size. Only two of the three children had histopathology available for review. No other cases of pulmonary hypertension were used as comparison and it is likely that other causes of pulmonary hypertension could result in similar imaging findings.

Conclusion

Our study describes the CT findings of three children with pulmonary hypertension caused by *BMPR2* mutations. All of children demonstrated similar findings of ground-glass nodules with prominent central vessels as well as dilated main bronchial arteries and transpleural pulmonary artery–to–bronchial artery anastomotic vessels. These findings correlated well with the pathological findings of diffuse plexogenic arteriopathy and pleural-based complex vascular lesions in the two children with pathology available for review. These findings support the previously reported histological evidence that plexogenic lesions act as shunts between the pulmonary artery and systemic bronchial circulations.

Declarations

Conflicts of interest Dr. Weinman is a reviewer of imaging studies in fibrosing lung disease for Parexel/Calyx and is on the advisory board and receives non-financial support from Boehringer Ingelheim for fi-

brosing lung disease. The University of Colorado School of Medicine has received consulting fees for Dr. Ivy from Actelion, Bayer, Gilead, Eli Lilly, Pfizer and United Therapeutics. Dr. Deterding is chief executive officer and founder of NowVitals Inc., founder and chief medical officer of Earables, coordinating investigator and consultant for Boehringer Ingelheim, and founder and consultant for EvoEndo. The other authors have nothing to disclose.

References

1. Berger RMF, Beghetti M, Humpl T et al (2012) Clinical features of paediatric pulmonary hypertension: a registry study. Lancet 379:537–546
2. Runo JR, Loyd JE (2003) Primary pulmonary hypertension. Lancet 361:1533–1544
3. Lane KB, Machado RD, Pauciulo MW et al (2000) Heterozygous germline mutations in BMPR2, encoding a TGF-beta receptor, cause familial primary pulmonary hypertension. Nat Genet 26:81–84
4. Evans JDW, Girerd B, Montani D et al (2016) BMPR2 mutations and survival in pulmonary arterial hypertension: an individual participant data meta-analysis. Lancet Respir Med 4:129–137
5. Heldin CH, Miyazono K, Ten Dijke P (1997) TGF-β signalling from cell membrane to nucleus through SMAD proteins. Nature 390:465–471
6. Morrell NW (2006) Pulmonary hypertension due to BMPR2 mutation: a new paradigm for tissue remodeling? Proc Am Thorac Soc 3:680–686
7. Croix CMS, Steinhorn RH (2016) New thoughts about the origin of plexiform lesions. Am J Respir Crit Care Med 193:484–485
8. Grosse C, Grosse A (2010) CT findings in diseases associated with pulmonary hypertension: a current review. Radiographics 30:1753–1777
9. Compton GL, Florence J, MacDonald C et al (2015) Main pulmonary artery–to–ascending aorta diameter ratio in healthy children on MDCT. AJR Am J Roentgenol 205:1322–1325
10. Brody AS, Guillerman RP, Hay TC et al (2010) Neuroendocrine cell hyperplasia of infancy: diagnosis with high-resolution CT. AJR Am J Roentgenol 194:238–244
11. Weinman JP, Manning DA, Liptzin DR et al (2017) HRCT findings of childhood follicular bronchiolitis. Pediatr Radiol 47:1759–1765
12. Weinman JP, White CJ, Liptzin DR et al (2018) High-resolution CT findings of pulmonary interstitial glycogenosis. Pediatr Radiol 48:1066–1072
13. LeMoine BD, Browne LP, Liptzin DR et al (2019) High-resolution computed tomography findings of thyroid transcription factor 1 deficiency (NKX2–1 mutations). Pediatr Radiol 49:869–875
14. Galambos C, Sims-Lucas S, Abman SH, Cool CD (2016) Intrapulmonary bronchopulmonary anastomoses and plexiform lesions in idiopathic pulmonary arterial hypertension. Am J Respir Crit Care Med 193:574–576
15. Townsley MI (2013) Structure and composition of pulmonary arteries, capillaries and veins. Compr Physiol 2:675–709
16. Oshima K, Crockett ES, Joshi SR et al (2019) Aneurysm-type plexiform lesions form in supernumerary arteries in pulmonary arterial hypertension: potential therapeutic implications. Am J Physiol Lung Cell Mol Physiol 317:L805–L815
17. Westöö C, Norvik C, Peruzzi N et al (2021) Distinct types of plexiform lesions identified by synchrotron-based phase contrast micro-CT. Am J Physiol Cell Mol Physiol 321:L17–L28
18. Rodríguez-Roisin R, Krowka MJ, Hervé P, Fallon MB (2004) Pulmonary-hepatic vascular disorders (PHD). Eur Respir J 24:861–880
19. Aldenkortt F, Aldenkortt M, Caviezel L et al (2014) Portopulmonary hypertension and hepatopulmonary syndrome. World J Gastroenterol 20:8072–8081
20. Ghigna MR, Guignabert C, Montani D et al (2016) BMPR2 mutation status influences bronchial vascular changes in pulmonary arterial hypertension. Eur Respir J 48:1668–1681